The susceptibility of an amino substituted triarylmethane dye towards the nucleophilic and electrophilic attack of peracids: the disparate kinetic effects of β-cyclodextrin

Alexei U. Moozyckine,[a] Pierre-Henri d'Hausen,[b] Christopher N. Tait[b] and D. Martin Davies*[b]

[a] *Department of Chemistry, University of Wales Swansea, Swansea, UK SA2 8PP*
[b] *Division of Chemical Sciences, School of Applied Sciences, Northumbria University, Newcastle upon Tyne, UK NE1 8ST*

Received (in Cambridge, UK) 14th August 2002, Accepted 24th September 2002
First published as an Advance Article on the web 1st November 2002

The kinetics of the oxidation of the *N,N*-dimethylamino substituted triarylmethane dye, Green S, by Caro's acid have been measured over a wide range of pH in the presence, where necessary, of the free radical scavenger, *N*-*tert*-butyl-α-phenylnitrone. The rate constants for the reaction of the dianionic form of the dye, $\mathbf{D}^{2-}$, and $^{-}OOSO_3^{-}$ is 3.5×10^{-2} $dm^3\ mol^{-1}\ s^{-1}$. Rate constants for the reactions of $\mathbf{D}^{2-}$ and $^{-}OOSO_3^{-}$ associated with one, two and three protons, respectively, have been determined, and from UV/visible spectral evidence for electrophilic attack of the peroxide on the tertiary amino group of the dye, assigned to the reactions of $\mathbf{D}^{2-}$ and $HOOSO_3^{-}$ ($1.8\ dm^3\ mol^{-1}\ s^{-1}$), $H\mathbf{D}^{-}$ and $HOOSO_3^{-}$ ($0.41\ dm^3\ mol^{-1}\ s^{-1}$), and $H\mathbf{D}^{-}$ and $HOOSO_3H$ ($5.9 \times 10^2\ K_{C2}\ dm^3\ mol^{-1}\ s^{-1}$, where K_{C2} is the first acid dissociation constant of $HOOSO_3H$). In contrast, spectral evidence shows that peracetic acid attacks the central carbon of the dye. The effect of β-cyclodextrin on the oxidation of Green S by peracetic acid shows a rate maximum with increasing cyclodextrin concentration. On the other hand, the oxidation by Caro's acid of one of the two tertiary amine nitrogen atoms of the dye is strongly inhibited at the lower concentrations of cyclodextrin and no further inhibition is observed at higher concentrations. The results are interpreted using the transition state pseudo-equilibrium constant approach. They are consistent with pathways involving the binding of both one and two molecules of cyclodextrin to the dye, where the orientation of the cyclodextrin is discussed in terms of simple field effects.

Introduction

Cyclodextrins are cyclic carbohydrate oligomers enzymatically produced from starch. β-Cyclodextrin consists of seven α-(1–4) linked D-glucopyranose units in a chair conformation, forming a hollow truncated cone with a hydrophilic exterior and a hydrophobic cavity, suitable for accommodating most simple aromatic guests.[1] Cyclodextrins are renowned for their propensity to form inclusion complexes with wide range of guest molecules.[2] This complex formation often becomes an important factor that influences the kinetics of the guest's reactions with other substances. Although many reactions affected by the presence of cyclodextrin in solution show simple saturation kinetics, some of them can be more complicated and in such cases a detailed kinetic analysis is needed to reveal the mechanism of catalysis or inhibition by the cyclodextrin host. Green S is a triarylmethane dye from the Victoria Blue family, whose distinctive feature is a hydroxyl positioned *ortho* to the central carbon of the dye. The bleaching of Green S by aqueous hydrogen peroxide or by water in alkali solution involves nucleophilic attack on the sp^2 hybridized central carbon of the dye *via* intramolecular base catalysis by the ionized *ortho*-hydroxyl.[3]

A recent paper demonstrated that with increasing β-cyclodextrin concentration the reaction of Green S with hydrogen peroxide is first accelerated and then slowed down.[4] This rate maximum is clear evidence for reaction pathways involving both one and two molecules of cyclodextrin and is interpreted as follows. The first cyclodextrin binds to an aryl group of the dye with the central carbon in a position where the field effect of the cyclodextrin attracts the nucleophilic oxygen atom of hydrogen peroxide and accelerates the reaction. The second cyclodextrin binds to another aryl group so as to sterically hinder the approach of hydrogen peroxide to the central carbon and slows down the reaction. Alkali bleaching of the dye is also accelerated by cyclodextrin, and the reverse reaction is slowed down, but no rate maxima or minima are observed. These results are also consistent with pathways involving both one and two molecules of cyclodextrin provided the second cyclodextrin stabilizes Green S and its alkali bleaching product to the same extent. The present paper shows that peracetic acid, like hydrogen peroxide, attacks the central carbon of Green S. Caro's acid, on the other hand, behaves as an electrophile and attacks a tertiary amine nitrogen atom of the dye. The effect of β-cyclodextrin on the reaction of peracetic acid is very similar to that of hydrogen peroxide whereas its effect on the reaction of Caro's acid is completely different.

Experimental

Green S (Lissamine Green B, Acid Green 50, Wool Green S, C.I. 44090), β-cyclodextrin, and other reagents used for preparing buffers were detailed previously.[3,4] Caro's acid in the form of the potassium peroxomonosulfate triple salt, $2\ KHSO_5 \cdot KHSO_4 \cdot K_2SO_4$ (Oxone®), peracetic acid and *N*-*tert*-butyl-α-phenylnitrone (*N*-benzylidene-*tert*-butylamine *N*-oxide), used with some runs as a free radical scavenger, were obtained from Aldrich. The peracetic acid was used after first removing the hydrogen peroxide impurity. This was done by raising the pH of a diluted solution to 9.8 for five minutes before adjusting to the working pH.[5] The absence of hydrogen peroxide in the peracid stock solutions was confirmed using a spectrophotometric method[6] employing a 15 % w/v solution of titanium(IV) sulfate purchased from Fisher. The ionic strength of the reaction

 DOI: 10.1039/b207931c

solutions was 0.10 mol dm^{-3}. The concentration of Green S was in the region of 1×10^{-5} mol dm^{-3} for the kinetic runs. The dye does not undergo any aggregation processes in the spectrophotometrically feasible range of concentrations and therefore the rate constant is independent of dye concentration.[3] Caro's acid concentrations ranged from 5.0×10^{-4} to 5.0×10^{-3} mol dm^{-3} and peracetic acid 1.2×10^{-4} to 2.0×10^{-3}. The UV/vis spectra were obtained using a Pharmacia Biotech Ultraspec 2000 instrument, fitted with a thermostatic cell-holder, and an Applied Photophysics SX-17MV stopped-flow spectrophotometer. For the pH measurements a Metrohm 702 SM Titrino was used. The solutions of Green S used at high pH values were fully equilibrated with respect to reversible alkali bleaching (which was slow compared to the peroxide bleaching reactions) prior to kinetic runs. All measurements were conducted at a temperature of 25.0 ± 0.2 °C. The reactions were generally followed at a wavelength corresponding to the maximum of the major absorbance peak of Green S at the particular pH. Pseudo-first-order rate constants were determined from plots of the logarithm of the absorbance change *versus* time for peracetic acid, and from the quotient of the initial rate of absorbance change and the initial absorbance,[7] for the Caro's acid bleaching of Green S. For each pH, rate constants were measured typically for at least six different concentrations of peracid. The observed second-order rate constants were calculated from the quotient of the pseudo-first-order rate constants and peracid concentration.

Results

Fig. 1 shows changes in the absorption spectrum of Green S during Caro's acid bleaching at pH 3.0. Initially, Fig. 1a, the main visible band at *ca.* 636 nm falls and there is an increase in absorbance over a wide range of wavelengths with isosbestic points at 544 nm and 321 nm. Other isosbestic points appear at 284 nm, 246 nm and 225 nm. The same pattern of spectral changes occurs during dye bleaching at pH 4.5 (not shown). The second stage of Caro's acid bleaching of Green S, Fig. 1b, shows a drop in absorbance at wavelengths over a large range of wavelengths above 309 nm and two other isosbestic points at 248 and 227 nm. The third time-resolved process, Fig. 1c, shows three isosbestic points at 358 nm, 308 nm and 217 nm. For the final stage, Fig. 1d, no isosbestic points occur during the disappearance of the peaks at *ca.* 239 nm and 333 nm. Rate constants estimated from the initial rate for the first stage, or log plots for the subsequent stages, are 4.7×10^{-3} s^{-1}, 1.1×10^{-3} s^{-1}, 6.1×10^{-4} s^{-1} and 1.8×10^{-5} s^{-1} for 5.0×10^{-4} mol dm^{-3} Caro's acid at pH 3.0. Fig. 2 shows the changes in the absorbance spectrum of the dye during Caro's acid bleaching at pH 8.5. Initially, Fig. 2a, the absorbance of the main visible band falls and there is an increase of absorbance at lower visible wavelengths with isosbestic points at 486 nm and 406 nm. The band at *ca*. 397 nm, that is not present at pH 3, shows a small drop whilst that at *ca*. 308 nm shows a more pronounced fall. The second stage, Fig. 2b, involves a drop in absorbance over the whole wavelength range. Similar spectral changes are observed at pH 10.5 (results not shown). Rate constants estimated from the initial rate for the first stage, or a log plot for the second are 9.9×10^{-3} s^{-1} and 1.5×10^{-3} s^{-1} for 5.0×10^{-3} mol dm^{-3} Caro's acid at pH 8.5. Fig. 3 shows the change in the absorbance spectrum during bleaching by peracetic acid at pH 8.5. Initially, Fig. 3a, the main visible band and that at *ca*. 398 nm fall and there is an increase in absorbance in the UV region, with approximate isosbestic points at 378 nm and 330 nm. The second stage, Fig. 3b, involves a drop in the remaining UV bands. Rate constants estimated from log plots at appropriate wavelengths are 7.1×10^{-3} s^{-1} for the first stage and 3.7×10^{-4} s^{-1} for the second, with 2.0×10^{-3} mol dm^{-3} peracetic acid.

The pH dependence of the of the initial stage of the Caro's acid bleaching of Green S is shown in Fig. 4. Addition

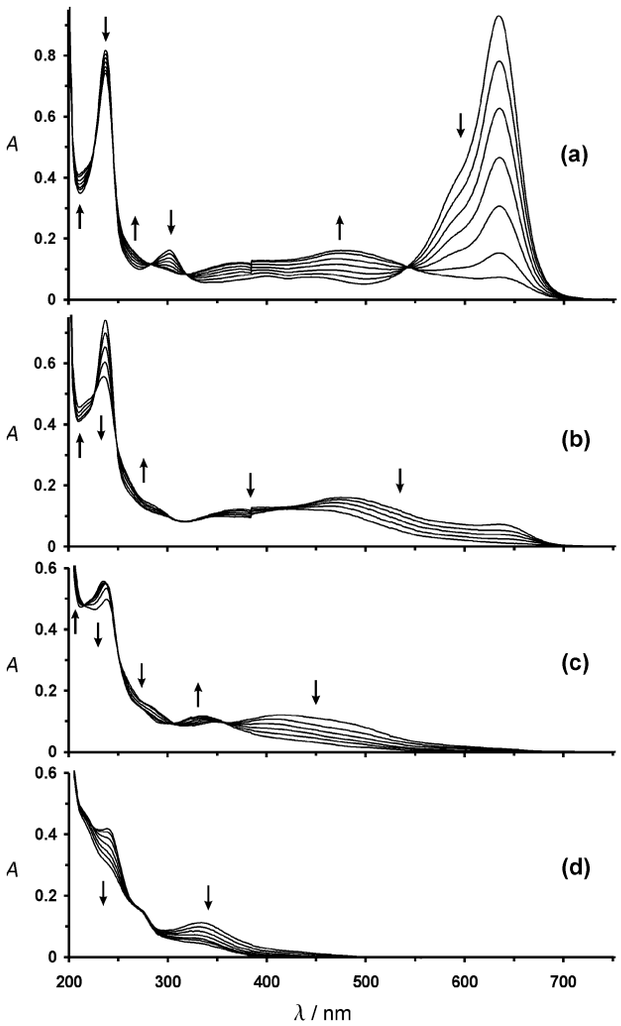

Fig. 1 Changes in the absorption spectrum of 1.25×10^{-5} mol dm^{-3} Green S during bleaching with 5.0×10^{-4} mol dm^{-3} Caro's acid at pH 3.0, ionic strength 0.10 mol dm^{-3}, 25 °C. Arrows indicate the direction of movement. Measurements made at the following times in minutes: (a) 0.2, 0.8, 1.4, 2.0, 2.6, 3.2, 3.6; (b) 3.6, 4.4, 5.2, 6.2, 8.0; (c) 10, 15, 20, 26, 32, 39; (d) 60, 100, 180, 300, 440, 580, 780.

of 5.0×10^{-4} mol dm^{-3} *N-tert*-butyl-α-phenylnitrone, an effective radical scavenger,[8] to runs at the lower pH values considerably decreased the reaction rate. The logarithmic plots of absorbance against time for the initial stage of Caro's acid bleaching of Green S exhibit a relatively small negative deviation from linearity, therefore we used the initial rates method in order to obtain more consistent values for first-order rate constants. The reaction scheme for Caro's acid (non-radical) interaction with Green S is shown in eqns. (1) to (9).

$$\mathbf{D}^{2-} + {}^{-}OOSO_3^- \xrightarrow{k_C^D} \text{Products} \quad (1)$$

$$\mathbf{D}^{2-} + HOOSO_3^- \xrightarrow{k_{C1}^D} \text{Products} \quad (2)$$

$$H\mathbf{D}^{-} + {}^{-}OOSO_3^- \xrightarrow{k_C^{D1}} \text{Products} \quad (3)$$

$$\mathbf{D}^{2-} + HOOSO_3H \xrightarrow{k_{C2}^D} \text{Products} \quad (4)$$

$$H\mathbf{D}^{-} + HOOSO_3^- \xrightarrow{k_{C1}^{D1}} \text{Products} \quad (5)$$

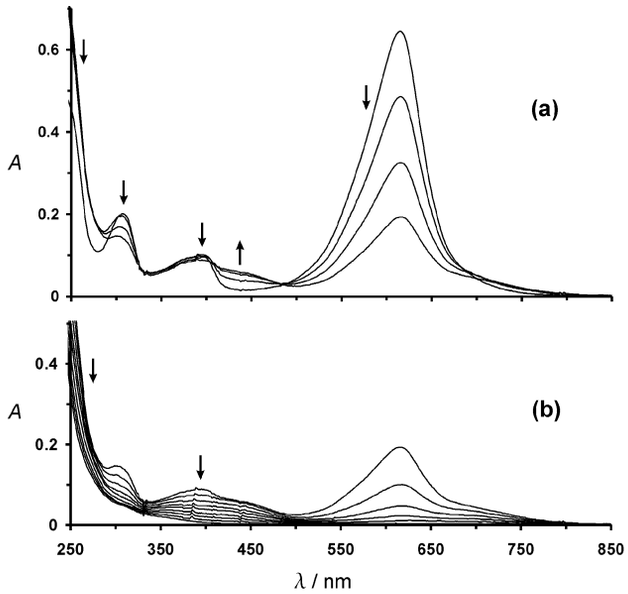

Fig. 2 Changes in the absorption spectrum of 1.25×10^{-5} mol dm^{-3} Green S during bleaching with 5.0×10^{-3} mol dm^{-3} Caro's acid at pH 8.5, ionic strength 0.10 mol dm^{-3}, 25 °C. Arrows indicate the direction of movement. Measurements made at the following times in minutes: (a) 0, 0.5, 1.0, 1.5; (b) 1.5, 2.0, 2.5, 3.0, 3.5, 4.5, 7.0, 11.5, 20.0.

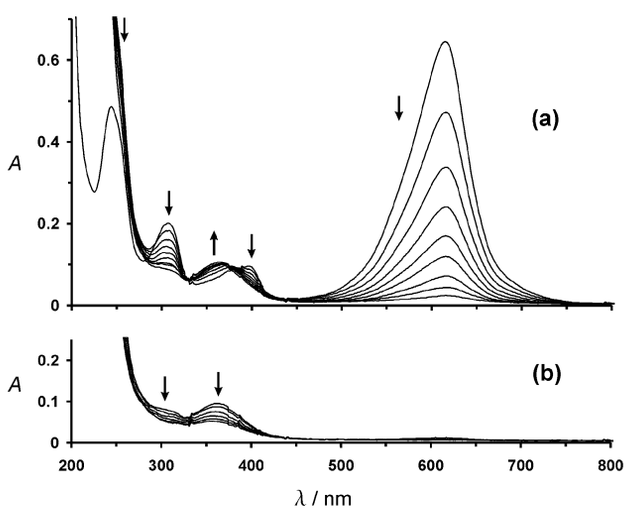

Fig. 3 Changes in the absorption spectra of 1.25×10^{-5} mol dm^{-3} Green S during bleaching with 2.0×10^{-3} mol dm^{-3} peracetic acid at pH 8.5, ionic strength 0.10 mol dm^{-3}, 25 °C. Arrows indicate the direction of movement. Measurements made at the following times in minutes: (a) 0, 0.8, 1.6, 2.4, 3.2, 4.0, 5.2, 7.0, 9.0; (b) 12, 15, 22, 29, 35, 40.

$$\mathrm{H_2D} + {}^{-}\mathrm{OOSO_3^-} \xrightarrow{k_C^{D2}} \text{Products} \quad (6)$$

$$\mathrm{HD^-} + \mathrm{HOOSO_3H} \xrightarrow{k_{C2}^{D1}} \text{Products} \quad (7)$$

$$\mathrm{H_2D} + \mathrm{HOOSO_3^-} \xrightarrow{k_{C1}^{D2}} \text{Products} \quad (8)$$

$$\mathrm{H_3D^+} + {}^{-}\mathrm{OOSO_3^-} \xrightarrow{k_C^{D3}} \text{Products} \quad (9)$$

The values of pK_a for Green S species, as shown in Scheme 1, are 7.66, pK_{D1} for $\mathbf{HD^-}$, and 1.31, pK_{D2} for $\mathbf{H_2D}$. The dye species $\mathbf{H_3D^+}$ is unidentifiable under the experimental conditions,[3] but the K_{D3} value for its acid dissociation to $\mathbf{H_2D}$ and H^+, which is necessary for kinetic considerations, is estimated to be at least 10 mol dm^{-3}. The Caro's acid dissociation equilibria are shown in eqns. (10) and (11). The pK_a value for the second dissociation constant, pK_{C1}, is 9.40.[9,10] That of the first, pK_{C2}, is < 0.[10]

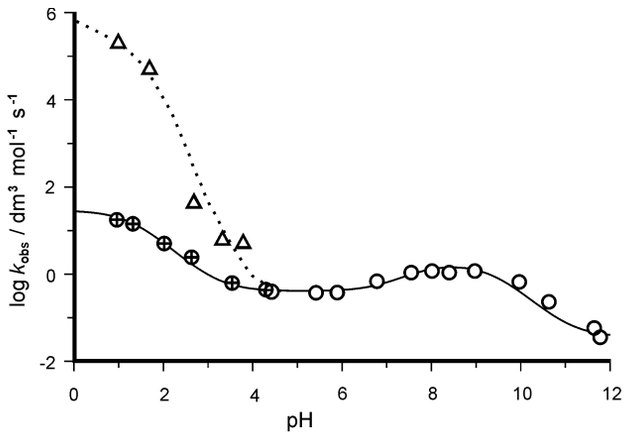

Fig. 4 The dependence upon pH of decimal logarithm of the observed second-order rate constant for Caro's acid bleaching of 1.25×10^{-5} mol dm^{-3} Green S at ionic strength 0.10 mol dm^{-3} and 25 °C. The crossed circles correspond to the points where free radical trapping agent, *N*-*tert*-butyl-α-phenylnitrone, has been added (5.0×10^{-4} mol dm^{-3}). The triangles represent the points where free radical trap has not been added to the reaction mixture. The solid curve represents the best fit of eqn. (12) to the data points (open and crossed circles); dotted curve shows the extent of free radical processes.

$$\mathrm{HOOSO_3H} \overset{K_{C2}}{\rightleftharpoons} \mathrm{HOOSO_3^-} + \mathrm{H^+} \quad (10)$$

$$\mathrm{HOOSO_3^-} \overset{K_{C1}}{\rightleftharpoons} {}^{-}\mathrm{OOSO_3^-} + \mathrm{H^+} \quad (11)$$

Following our previous treatment of the hydrogen peroxide reaction,[3] and since there are only three points of inflection for the pH dependence of k_{obs} shown in Fig. 4, k_{obs} is given by eqn. (12) where k_{0obs}, k_{1obs}, k_{2obs} and k_{3obs} are defined in eqns. (13)–(16). In all indexes (K_{Dn}, K_{Cn}, k_{Cn}^{Dn}) n corresponds to the number of protons.

$$k_{obs} = \frac{k_{0obs} + k_{1obs}[H^+] + k_{2obs}[H^+]^2 + k_{3obs}[H^+]^3}{K_{D1}K_{D2}K_{C1} + K_{D1}K_{D2}[H^+] + K_{D2}[H^+]^2 + [H^+]^3} \quad (12)$$

$$k_{0obs} = k_C^D K_{D1} K_{D2} K_{D3} K_{C1} \quad (13)$$

$$k_{1obs} = k_{C1}^D K_{D1} K_{D2} + k_C^{D1} K_{D2} K_{C1} \quad (14)$$

$$k_{2obs} = k_{C2}^D K_{D1} K_{D2}/K_{C2} + k_{C1}^{D1} K_{D2} + k_C^{D2} K_{C1} \quad (15)$$

$$k_{3obs} = k_{C2}^{D1} K_{D2}/K_{C2} + k_{C1}^{D2} + k_C^{D3} K_{C1}/K_{D3} \quad (16)$$

The best fit values of the kinetic parameters, k_{0obs} to k_{3obs}, and their standard deviations (shown in Table 1) were obtained using non-linear least squares data fit (k_{obs}) into eqn. (12) with proportional weighting; the solid curve corresponding to these best-fit values is shown in Fig. 4. The second-order rate constants given in Table 1 were calculated from eqns. (13)–(16), where k_C^D was determined unambiguously, and for the others the upper limits were calculated by assigning all but one rate constants in the equiproton sets to zero in turns, in the same way as before.[3]

Effect of cyclodextrin

The effects of cyclodextrin on the reactions of peracetic acid or Caro's acid and Green S are shown in Figs. 5 and 6, respectively. Following previous work,[4] the dependence of k_{obs}^X values on

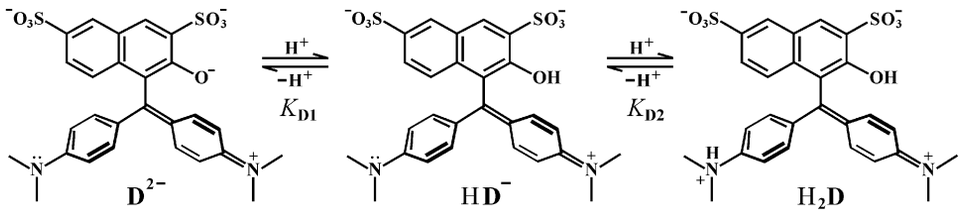

Scheme 1

Table 1 Observed rate constants ($dm^3\ mol^{-1})^{n+1}\ s^{-1}$ calculated for pathways involving n additional protons in the transition state and the corresponding upper limits for the bimolecular rate constants ($dm^3\ mol^{-1}\ s^{-1}$)

n	$k_{n\ obs}$	k_C^{Dn}	k_{C1}^{Dn-1}	k_{C2}^{Dn-2}
0	$(1.5 \pm 0.3) \times 10^{-20}$	3.5×10^{-2}		
1	$(1.9 \pm 0.3) \times 10^{-9}$	9.8×10^{1}	1.8×10^{0}	
2	$(2.0 \pm 0.3) \times 10^{-2}$	5.0×10^{7}	4.1×10^{-1}	$1.9 \times 10^{7}\ K_{C2}$
3	$(2.9 \pm 0.4) \times 10^{1}$	$7.3 \times 10^{10}\ K_{D3}$	2.9×10^{1}	$5.9 \times 10^{2}\ K_{C2}$

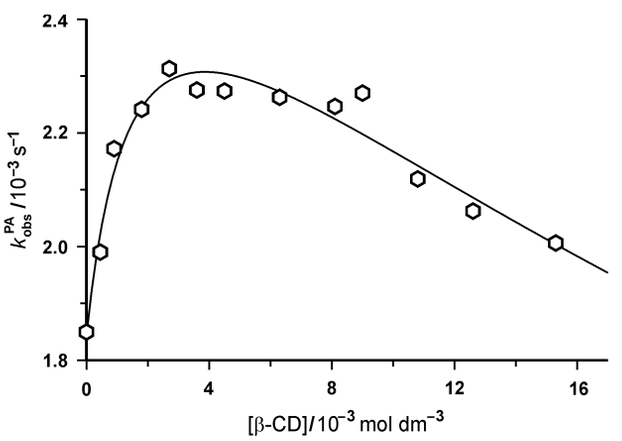

Fig. 5 Effect of cyclodextrin on the pseudo-first-order rate constant for reaction of Green S with 9.5×10^{-4} mol dm^{-3} peracetic acid in phosphate buffer, pH 8.2, ionic strength 0.1 mol dm^{-3}. The curve represents the best fit values of the parameters according to eqn. (17) with $K_{11}^{D}K_{12}^{D}$, 14000 $dm^6\ mol^{-2}$.

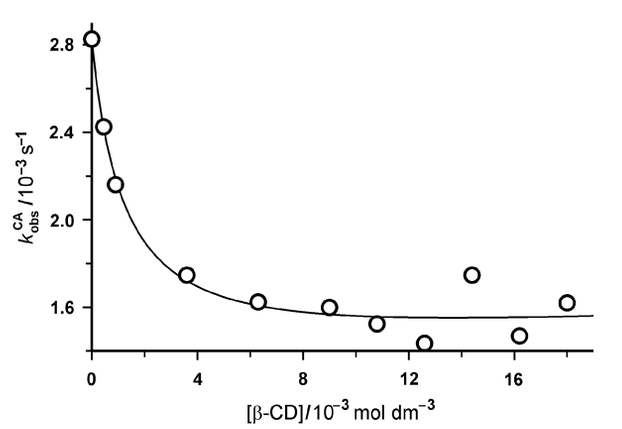

Fig. 6 Effect of cyclodextrin on the pseudo-first-order rate constants for reaction of Green S with 2.0×10^{-3} mol dm^{-3} Caro's acid in carbonate buffer, pH 9.8, ionic strength 0.1 mol dm^{-3}. Curve as in Fig. 5.

cyclodextrin concentration is described by eqn. (17) where X is an identity variable for the Green S reaction partner, either peracetic acid, PA, or Caro's acid, CA; the rate constants k_0^X, k_{1obs}^X and k_{2obs}^X are the respective zero-, first- and second-order dependencies on cyclodextrin concentration; K_{11}^D and K_{12}^D and are the respective 1:1 and 2:1 stepwise binding constants of the dye and cyclodextrin.

$$k_{obs}^{X} = \frac{k_0^X + k_{1obs}^X[CD] + k_{2obs}^X[CD]^2}{1 + K_{11}^D[CD] + K_{11}^D K_{12}^D[CD]^2} \quad (17)$$

As described previously for hydrogen peroxide,[4] it is not possible to fit the data for peracetic acid using all the parameters in eqn. (17) because the data points do not adequately define the form of the curve at high cyclodextrin concentration and are consistent both with a sharp decrease in k_{obs}^{PA} to a fairly high limiting value (*i.e.* relatively large K_{12}^D and k_{2obs}^{PA} compared to the 1:1 parameters) or a much more gradual decrease to a much lower limiting value (*i.e.* relatively small K_{12}^D and k_{2obs}^{PA}). Hence we are constrained to exploring the limits of eqn. (17) at chosen constant values of $K_{11}^D K_{12}^D$. For the purposes of comparing the effect of cyclodextrin on the various reactions it is sufficient to use a single value of $K_{11}^D K_{12}^D$, and Table 2 shows the best-fit values of the parameters when it is set to 14000 $dm^6\ mol^{-2}$, the lower limit below which negative rate parameters are obtained.

Scheme 2 shows the thermodynamic cycles for the interaction

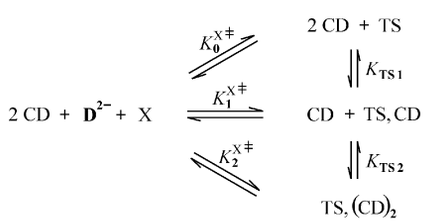

Scheme 2

of one and two molecules of cyclodextrin with the transition state formed by Green S and its reaction partner. Application of transition state theory to the cycles leads to eqns. (18) and (19) for the transition state pseudo-equilibrium constants,

$$K_{TS1} = \frac{K_1^{X\ddagger}}{K_0^{X\ddagger}} = \frac{k_{1\,obs}^X}{k_0^X} \quad (18)$$

$$K_{TS2} = \frac{K_2^{X\ddagger}}{K_1^{X\ddagger}} = \frac{k_{2\,obs}^X}{k_{1obs}^X} \quad (19)$$

K_{TS1} and K_{TS2}. Here, K_{TS1} represents the stabilization imparted to the transition state as a result of its association with one cyclodextrin molecule and K_{TS2} represents the additional stabilization or the destabilization imparted by a second cyclodextrin molecule. Table 3 includes the binding constants and transition state equilibrium constants derived from the data in Table 2 either directly or using eqns. (18) and (19).

Discussion

It is useful to compare the reactions of Green S and peracetic or Caro's acid with that of the dye and hydrogen peroxide since the effect of cyclodextrin on the latter reaction has already been described.[4] In the first place it is notable from Fig. 4 that below pH 4 there is a fast oxidation that is clearly a radical chain process since it is inhibited by the radical trapping agent,

Table 2 Best-fit values (± standard deviation) of binding constant and rate constants for $K_{11}^{D}K_{12}^{D}$, 14000 dm^6 mol^{-2}

X	K_{11}^{D}/dm^3 mol^{-1}	k_0^X/10^{-3} s^{-1}	k_{1obs}^X/dm^3 mol^{-1} s^{-1}	k_{2obs}^X/dm^6 mol^{-2} s^{-1}
CA	800 ± 500	2.82 ± 0.16	1.1 ± 0.8	29 ± 10
PA	600 ± 200	1.84 ± 0.03	1.6 ± 0.5	1 ± 5

Table 3 Binding constants and transition state pseudo-equilibrium constants (± standard deviation) for $K_{11}^{D}K_{12}^{D}$, 14000 dm^6 mol^{-2}

X	K_{11}^{D}/dm^3 mol^{-1}	K_{TS1}/dm^3 mol^{-1}	K_{12}^{D}/dm^3 mol^{-1}	K_{TS2}/dm^3 mol^{-1}
PA[a]	600 ± 200	870 ± 270	23 ± 8	0.6 ± 3
CA[a]	800 ± 500	390 ± 320	18 ± 11	26 ± 19
H_2O_2[b]	460 ± 120	890 ± 180	30 ± 8	0.3 ± 3
H_2O[b]	800 ± 170	1260 ± 210	18 ± 4	17 ± 4

[a] Present work. [b] From ref. 4.

N-*tert*-butyl-α-phenylnitrone.[8] Such a process is not apparent with hydrogen peroxide.[3,7] In the presence of the radical trap the spectral changes shown in Figs. 1a and 1b are very similar to those observed during and subsequent to the *N*-oxidation of Green S by $H_3O_2^+$, although on a much faster time scale.[7] We can safely conclude, therefore, that *N*-oxidation is the initial major reaction occurring between Green S and Caro's acid at low pH. In addition, further oxidation processes occur with Caro's acid that are not observed with hydrogen peroxide at low pH. The relative similarity of the rate constants for the first two processes accounts for the negative deviation observed in the log plots. At pH values where $\mathbf{D}^{2-}$ predominates, the spectral changes (Fig. 2) are still consistent with *N*-oxidation, rather than attack at the central carbon, which would destroy the conjugated system and abolish absorbance in the visible region, which is not the case.

Table 1 shows the values of $k_{n\ obs}$ obtained from the curve fitting of the data in Fig. 4 according to eqn. (12). When *n* is zero, this represents the reaction between $\mathbf{D}^{2-}$ and $^-OOSO_3^-$. When *n* is one, this represents the reaction of $\mathbf{D}^{2-}$ and $^-OOSO_3^-$ plus one additional proton, and so on. Table 1 shows the upper limits for the corresponding bimolecular rate constants calculated from the respective $k_{n\ obs}$ values according to eqns. (13)–(16). For the reaction involving three additional protons the value of k_C^{D3} is too far above the diffusion control limit, taking into account that $K_{D3} \geq 10$, for the reaction of $H_3\mathbf{D}^+$ and $^-OOSO_3^-$ to be feasible. Moreover, the reaction between $H_2\mathbf{D}$ and $HOOSO_3^-$ can be ruled out since the *N*-protonated species $H_2\mathbf{D}$ is incapable of forming an *N*-oxide, which is the main initial reaction product, as evidenced by Fig. 1a. Hence the predominant reaction at low pH must be that between $H\mathbf{D}^-$ and $HOOSO_3H$ with rate constant k_{C2}^{D1} where the value of the quantity K_{C2} is greater than 1 mol dm^{-3}.[10] For the reaction involving two additional protons the value of k_{C2}^{D} for the reaction of $\mathbf{D}^{2-}$ and $HOOSO_3H$ seems much too high compared with the value of k_{C2}^{D1} considered previously and is bordering on the diffusion controlled limit. Equally, the rate constant shown in Table 1 for the reaction of $H_2\mathbf{D}$ and $^-OOSO_3^-$ is bordering on the diffusion control limit and, moreover, can be ruled out since this dye species is incapable of forming the *N*-oxide. Therefore the reaction between $H\mathbf{D}^-$ and $HOOSO_3^-$ must predominate and the value of k_{C1}^{D1} is significantly less than that of k_{C2}^{D1} due to the repulsion between the like-charged reactants in the former case. The reaction involving one additional proton also involves *N*-oxidation, as evidenced by the spectral changes at higher pH, Fig. 2. Hence the reaction between $\mathbf{D}^{2-}$ and $HOOSO_3^-$ predominates because nucleophilic attack of $H\mathbf{D}^-$ on $^-OOSO_3^-$ would be expected to be slower than that of $H\mathbf{D}^-$ on $HOOSO_3^-$ and the calculated upper limit value of k_C^{D1} in Table 1 is in fact actually greater than that of k_{C1}^{D1} accepted for the reaction of the monoanion of Caro's acid. The value of k_{0obs} is so small that at pH 10.5 the reaction involving the protonated species still predominates. The value of k_{0obs} does lead to the unambiguous assignment of k_C^D, however, and we believe that, because of its value, this rate constant represents nucleophilic attack of the Caro's acid dianion on the central carbon of $\mathbf{D}^{2-}$. It is *ca*. ten times less than the value, 3.1×10^{-1} dm^3 mol^{-1} s^{-1}, reported for the reaction of HO_2^- and $\mathbf{D}^{2-}$,[3] and this is about the same ratio of rate constants as that of the two nucleophiles with acetyloxybenzenesulfonate.[11]

The reaction of peracetic acid and Green S at pH 8.5 shown in Fig. 3, by contrast to that of peroxomonosulfate at pH 8.5, is virtually identical to that of hydrogen peroxide at the same pH.[7] As in the latter case, the complete loss of visible absorbance is commensurate with loss of the conjugated system around the central carbon. In the case of peracetic acid, attack at the tertiary nitrogen is not expected compared with $H_3O_2^+$ and $HOOSO_3^-$ because the leaving group character of acetate (pK_a of acetic acid, 4.7) is much less than that of water (pK_a of H_3O^+, −1.7) and sulfate (pK_a of $HOSO_3^-$, 2.0). A linear relationship exists between the logarithm of the rate constant for electrophilic reactions and the pK_a of the conjugate acid of the leaving group for a range of peroxides including the aforementioned,[12] and likewise for peracids and tertiary amines.[13]

Effect of cyclodextrin

It is known that the binding of peracetic acid and Caro's acid to α-cyclodextrin is very weak or undetectable.[14] The reasonable assumption has been made in the treatment of the present data (where there are no terms in peroxide binding constants in the denominator of eqn. (17)) that this is also the case for β-cyclodextrin. The rate maximum for the effect of cyclodextrin on the reaction of peracetic acid and Green S shown in Fig. 5 is clear evidence for reaction pathways involving both one and two molecules of cyclodextrin and this is interpreted in terms of the existence of both 1:1 and 2:1 complexes of β-cyclodextrin and the dye. A similar interpretation was made in the case of hydrogen peroxide.[4] The reaction of Caro's acid and Green S, Fig. 6, does not appear to be influenced markedly at higher cyclodextrin concentrations. A similar observation was made for the forward and reverse reactions of alkali bleaching of the dye, and was interpreted in terms of the second cyclodextrin stabilizing the reactant and product to the same extent.[4] For the irreversible oxidation of the dye by Caro's acid it will be shown that the second cyclodextrin stabilizes the dye and the transition state to the same extent. The second cyclodextrin molecule, therefore, performs no catalytic or inhibitory function. We have previously reported a similar situation where binding of a second cyclodextrin to 4-*tert*-butylperbenzoic, peroctanoic, and pernonanoic acids stabilizes these peracids to the same extent as their transition states for reaction with aryl alkyl sulfides. We have suggested that this be termed 'neutral binding' as opposed to 'non-productive binding' where the cyclodextrin field inhibits the reaction.[15]

A complicating factor, due to the limited solubility of the cyclodextrin, is that measurements cannot be made at high enough concentrations to define the 2:1 binding constant precisely. Curve fitting is therefore carried out using the lower limit of the product of the 1:1 and 2:1 binding constants of the cyclodextrin and Green S, $K_{11}^{D}K_{12}^{D}$, 14000 $dm^6\ mol^{-2}$, obtained from the reaction with peracetic acid. This lower limit is the same as that obtained previously with hydrogen peroxide.[4] A single value of the product $K_{11}^{D}K_{12}^{D}$ is considered for the sake of simplicity. Use of a reasonable upper limit of $K_{11}^{D}K_{12}^{D}$, 100000 $dm^6\ mol^{-2}$, does not alter the conclusions (results not shown).

For comparative purposes, the kinetic and equilibrium parameters in Table 2 are best considered in terms of transition state pseudo-equilibrium constants. This approach was originally developed for acid–base catalysis by Kurz, it has also been used to discuss enzyme catalysis and has been adapted by Tee for reactions mediated by cyclodextrins and other systems such as surfactant micelles.[16–18] In this paper the triangular thermodynamic cycles of Scheme 2 differ in form but not in principle [16] from the more usual rectangular cycles that would include the binding constants of the dye and cyclodextrin, K_{11}^{D} and K_{12}^{D}. Analogous triangular cycles have been used previously for the cyclodextrin mediated reactions of peroxides with organic sulfides and *p*-nitrophenyl acetate.[15,19] The usefulness of the triangular cycles is that they lead directly to values of the transition state equilibrium constants, K_{TS1} and K_{TS2}, *via* the ratios of rate constants given in eqns. (5) and (6) and these can be compared with values of the binding constants K_{11}^{D} and K_{12}^{D}. Thus the magnitude of K_{TS1} compared with K_{11}^{D} provides a quantitative comparison of the stabilization of the transition state and the dye by a molecule of cyclodextrin that is independent of any prior assumptions about the mechanism of catalysis or inhibition.

Table 3 shows the binding constants and transition state pseudo-equilibrium constants, obtained as described in the results section for the peracetic acid and Caro's acid reactions, together with the corresponding values previously reported for hydrogen peroxide and alkali bleaching. It is a measure of the self-consistency of the results that the values of the 1:1 and 2:1 binding constants for the dye and cyclodextrin, K_{11}^{D} and K_{12}^{D} respectively, are in agreement within 1.3 standard deviations and that seven out of the eight values agree within one standard deviation, which is all that should be expected on statistical grounds.

Field effects

Cyclodextrin field effects are those where the cyclodextrin influences the reactivity of molecules, not by forming covalent bonds, but *via* the intermolecular forces, which are, numbered in order of increasing range: (i) repulsion (*i.e.* steric), (ii) dispersion, dipole–(induced dipole), dipole–dipole, (iii) ion–(induced dipole), (iv) ion–dipole, and (v) ion–ion. Field effects in cyclodextrin-mediated reactions have recently been reviewed.[20]

Fig. 5 shows that the reaction of peracetic acid is first accelerated then slowed down with increasing concentrations of cyclodextrin, and Table 3 allows a quantitative comparison with the similar effect observed previously with hydrogen peroxide. The similarity of the K_{TS1} and K_{TS2} values for these two oxidants shows that the first and second molecules of cyclodextrin are having exactly the same effect on the two transition states. This is expected since both oxidants attack the central carbon of Green S. The field effects due to the cyclodextrin molecule or molecules in the hydrogen peroxide reaction were discussed in an earlier paper,[4] and the same reasoning applies with peracetic acid. In the 1:1 complex the $(CH_3)_2NC_6H_4$ moiety of the dye is included in the cyclodextrin cavity leaving the central carbon of the dye in a position where the field effect attracts the nucleophilic oxygen atom of the peroxides and accelerates the reaction. It is suggested that the orientation of β-cyclodextrin so that the narrow end of its cavity is adjacent to the central carbon of Green S, with the electron-donating dimethylamine substituent at the wider end of the cavity is that expected from the field effect of the overall dipole of the cyclodextrin molecule. This orientation is feasible from consideration of space filling models,[4] (in Scheme 3, the structure on the

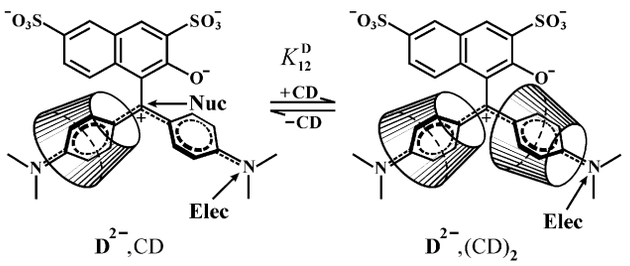

Scheme 3

left of the equilibrium is a schematic representation) and the cyclodextrin dipole would provide the field required for the observed rate acceleration for the reactions of nucleophiles and the 1:1 cyclodextrin–dye complex. In the 2:1 complex both cyclodextrin molecules bind to aryl moieties of the dye and this causes steric hindrance for the approach of the peroxides to the central carbon, resulting in the observed rate deceleration of the reactions at higher cyclodextrin concentrations.

The very different effect of cyclodextrin on the electrophilic attack of Caro's acid on the nucleophilic nitrogen atoms of the $(CH_3)_2NC_6H_4$ moieties of Green S, Fig. 6, will now be considered. Table 3 shows that for Caro's acid K_{TS1} is approximately half K_{11}^{D}, showing that the reaction is approximately 50% inhibited by one molecule of cyclodextrin. This represents very strong inhibition since the dye has two $(CH_3)_2NC_6H_4$ moieties. In marked contrast to this, consideration of K_{TS2} and K_{12}^{D} shows that the second cyclodextrin certainly does not inhibit the reaction further and may actually slightly accelerate it. The possible explanation that the second cyclodextrin binds to the naphthyl moiety of the dye can be rejected since space-filling molecular models show that one of the charged sulfonate groups would be located deep inside the cyclodextrin cavity, which would involve an unfavourable desolvation energy. Most probably, the second cyclodextrin also binds to a $(CH_3)_2NC_6H_4$ moiety so that the narrow end of at least one cyclodextrin cavity is adjacent to the central carbon of the dye, otherwise the dye would be too far inside one cyclodextrin cavity to be able to bind to the other. The different orientations of the two cyclodextrins with respect to the tertiary amine reaction partner of the Caro's acid anion provides the key to the very different effects of 1:1 and 2:1 binding, this is illustrated in Scheme 3. In the 1:1 complex, with the dimethylamine substituent at the wide end of the cavity as suggested in the previous paragraph, the overall dipole of the cyclodextrin molecule repels the Caro's acid anion at relatively long range (compared, for example, to dipole–dipole forces important in determining the orientation of reactants in the transition state) and strongly inhibits the reaction to the maximum possible extent, which is 50%. When a second cyclodextrin molecule is bound to the dye with the dimethylamine substituent at the narrower end of the cyclodextrin, the favourable ion–dipole attraction more or less compensates for any steric constraints imposed upon the Caro's acid and there is no further inhibition.

References

1 J. Szejtli, *Chem. Rev.*, 1998, **98**, 1743.
2 K. A. Connors, *Chem. Rev.*, 1997, **97**, 1325.
3 D. M. Davies and A. U. Moozyckine, *J. Chem. Soc., Perkin Trans. 2*, 2000, 1495.
4 P.-H. d'Hausen, C. N. Tait and D. M. Davies, *J. Chem. Soc., Perkin Trans. 2*, 2002, 398.

5 D. M. Davies and M. E. Deary, *J. Chem. Res. (M)*, 1988, 2720.
6 (*a*) N. L. Gil-Ad and A. M. Mayer, *FEMS Microbiol. Lett.*, 1999, **176**, 455; (*b*) F. D. Snell and C. T. Snell, *Colorimetric Methods of Analysis*, Vol. II, D. Van Nostrand Co., New York, 1949; (*c*) G. M. Eisenberg, *Ind. Eng. Chem., Anal. Ed.*, 1943, **15**, 327.
7 A. U. Moozyckine and D. M. Davies, *Green Chem.*, 2002, **4**, 452.
8 (*a*) K. M. Thompson, M. Spiro and W. P. Griffith, *J. Chem. Soc., Faraday Trans.*, 1996, 2535; (*b*) K. M. Thompson, W. P. Griffith and M. Spiro, *J. Chem. Soc., Faraday Trans.*, 1994, 1105; (*c*) K. M. Thompson, W. P. Griffith and M. Spiro, *J. Chem. Soc., Faraday Trans.*, 1993, 1203; (*d*) K. M. Thompson, W. P. Griffith and M. Spiro, *J. Chem. Soc., Chem. Commun.*, 1992, 1600.
9 A. Lange, M. Hild and H.-D. Brauer, *J. Chem. Soc., Perkin Trans. 2*, 1999, 1343.
10 L. B. Brasileiro, J. L. Colodette and D. Piló-Veloso, *Quim. Nova*, 2001, **24**, 819.
11 D. M. Davies, S. J. Foggo and P. M. Paradis, *J. Chem. Soc., Perkin Trans. 2*, 1998, 1381.
12 (*a*) R. Curci and J. O. Edwards in *Organic Peroxides*, ed. D. Swern, Wiley Interscience, New York, 1970, vol. 1, pp. 218–240; (*b*) B. Plesnicar in *The Chemistry of Functional Groups, Peroxides*, ed. S. Patai, John Wiley and Sons Ltd., New York, 1983, pp. 522–524, 539–540.
13 D. M. Davies and R. M. Jones, *J. Chem. Soc., Perkin Trans. 2*, 1989, 1323.
14 D. M. Davies and M. E. Deary, *J. Chem. Soc., Perkin Trans. 2*, 1996, 2415.
15 D. M. Davies and M. E. Deary, *J. Chem. Soc., Perkin Trans. 2*, 1996, 2423.
16 (*a*) J. L. Kurz, *J. Am. Chem. Soc.*, 1963, **85**, 987; (*b*) J. L. Kurz, *Acc. Chem. Res.*, 1972, **5**, 1.
17 (*a*) J. Kraut, *Science*, 1988, **242**, 533; (*b*) A. J. Kirby, *Angew. Chem., Int. Ed. Engl.*, 1996, **35**, 707; (*c*) S. J. Eustace, G. M. McCann, R. A. More O'Ferrall, M. G. Murphy, B. A. Murray and S. M. Walsh, *J. Phys. Org. Chem.*, 1998, **11**, 519.
18 (*a*) O. S. Tee, *Carbohydr. Res.*, 1989, **192**, 181; (*b*) O. S. Tee, *Adv. Phys. Org. Chem.*, 1994, **29**, 1; (*c*) O. S. Tee and O. J. Yazbeck, *Can. J. Chem.*, 2000, **78**, 1100.
19 D. M. Davies and M. E. Deary, *J. Chem. Soc., Perkin Trans. 2*, 1999, 1027.
20 K. Takahashi, *Chem. Rev.*, 1998, **98**, 2013.